Anticancer activity of the supercritical extract of Brazilian green propolis and its active component, artepillin C: Bioinformatics and experimental analyses of its mechanisms of action

PRIYANSHU BHARGAVA[1,2*], ABHINAV GROVER[3*], NUPUR NIGAM[1*], ASHISH KAUL[1,4], MOTOMICHI DOI[1,2], YOSHIYUKI ISHIDA[5], HANZO KAKUTA[6], SUNIL C. KAUL[1], KEIJI TERAO[5,7] and RENU WADHWA[1]

[1]DBT-AIST International Laboratory for Advanced Biomedicine (DAILAB), National Institute of Advanced Industrial Science and Technology (AIST), Tsukuba, Ibaraki 305 8565; [2]Graduate School of Life and Environmental Sciences, University of Tsukuba, Ibaraki 305 8575, Japan; [3]School of Biotechnology, Jawaharlal Nehru University, New Delhi 110 067, India; [4]School of Integrative and Global Majors, University of Tsukuba, Ibaraki 305 8577; [5]CycloChem Co., Ltd., Kobe 650 0047; [6]Fujimi Bee House Co., Ltd., Shiki 353 0003; [7]Graduate School of Medicine, Kobe University, Kobe 650 0017, Japan

Received August 6, 2017; Accepted December 13, 2017

DOI: 10.3892/ijo.2018.4249

Abstract. Propolis, a resinous substance collected by honeybees by mixing their saliva with plant sources, including tree bark and leaves and then mixed with secreted beeswax, possesses a variety of bioactivities. Whereas caffeic acid phenethyl ester (CAPE) has been recognized as a major bioactive ingredient in New Zealand propolis, Brazilian green propolis, on the other hand, possesses artepillin C (ARC). In this study, we report that, similar to CAPE, ARC docks into and abrogates mortalin-p53 complexes, causing the activation of p53 and the growth arrest of cancer cells. Cell viability assays using ARC and green propolis-supercritical extract (GPSE) revealed higher cytotoxicity in the latter, supported by nuclear translocation and the activation of p53. Furthermore, *in vivo* tumor suppression assays using nude mice, we found that GPSE and its conjugate with γ cyclodextrin (γCD) possessed more potent anticancer activity than purified ARC. GPSE-γCD may thus be recommended as a natural, effective and economic anticancer amalgam.

Correspondence to: Dr Renu Wadhwa, DBT-AIST International Laboratory for Advanced Biomedicine (DAILAB), National Institute of Advanced Industrial Science and Technology (AIST), Central 5-41, 1-1-1 Higashi, Tsukuba, Ibaraki 305 8565, Japan
E-mail: renu-wadhwa@aist.go.jp

Dr Keiji Terao, CycloChem Co., Ltd., 7-4-5 Minatojima-minamimachi, Chuo-ku, Kobe 650 0047, Japan
E-mail: keiji.terao@cyclochem.com

*Contributed equally

Abbreviations: ARC, artepillin C; GPSE, green propolis supercritical extract; γCD, γ cyclodextrin; DMEM, Dulbecco's modified Eagle's medium; CAPE, caffeic acid phenethyl ester; GADD45, growth arrest and DNA damage-inducible 45; MTT, 3-(4,5-dimethylthiazol-2-yl)-2, 5-diphenyltetrazolium bromide; BSA, bovine serum albumin; PBS, phosphate-buffered saline

Key words: Brazilian green propolis, supercritical extract, γ cyclodextrin conjugate, p53-mortalin complex, abrogation, anticancer

Introduction

Propolis is a complex mixture of resinous material, produced by bees, created by mixing their saliva with the botanical sources they live on. The color (yellowish green to dark brown) and odor (odorless to aromatic) of propolis vary and depend on its botanical source, origin of place and bee characteristics, such as strain and age (1,2). Apart from the structural and functional attributes of propolis for beehives (1), propolis has been reported to possess a variety of disease-preventive and therapeutic potentials for the human population (3). There are mainly two types of propolis known that differ in their constituents: New Zealand propolis that possesses caffeic acid phenethyl ester (CAPE) and Brazilian green propolis that possesses artepillin C (ARC) as predominant bioactive ingredients. Besides these, over 150 constituents, including flavonoids, phenolic acids, esters, terpenoids, steroids, amino acids and cinnamic acid derivatives have been identified (3), and are hence considered as popular pharmacological research material (4). A broad spectrum of biological activities identified in propolis include antitumor (5-12), anti-inflammatory (13-15), anti-bacterial (16-18), anti-viral (16,19,20) and anti-fungal (16) activities. Propolis is used in cosmetic products, such as body lotions, ointments, face creams and in functional food in various forms, such as tablets, capsules, toothpaste and mouthwash preparations (21). Molecular studies on the anticancer activity of propolis have revealed that its phenolic components cause cell cycle arrest and apoptosis (11), mitochondrial stress (22) and the inhibition of tumor growth (11,22,23). CAPE-based propolis extract (Bio-30) has been reported to block p21 (RAC1) activated

kinase 1 (PAK1) signalling and to suppress tumors in neurofibromatosis (9,24,25).

ARC (3,5-diprenyl-4-hydroxycinnamic acid) is one of the active phenolic acid components of Brazilian propolis generated by bees from materials from a Brazilian plant, *Baccharis dracunculifolia*. It has been shown to possess various biological activities, such as anti-viral (14), anti-bacterial (14,26), antioxidant (26) and anti-carcinogenic (14,26-28) activities. ARC has been reported to inhibit the growth of transplanted solid human and mouse tumors, including malignant melanoma in athymic and thymic mice, respectively (27). CAPE and ARC have been reported to differ in their bioavailability profile that in turn is determined by the stability of the compounds to the digestive enzymes and absorption through the intestinal lining. CAPE alone becomes degraded by secreted esterases (12); however, when combined with γ cyclodextrin (γCD) it is protected and has improved activity in *in vitro* and *in vivo* antitumor assays (12). On the other hand, ARC has been reported to possess extremely low absorption efficiency and bioavailability. Whereas CAPE is absorbed and distributed by the monocarboxylic acid transporter (MCT)-mediated transport system (29), ARC is mainly permeated across by transcellular passive diffusion (30). We previously performed a cDNA array of CAPE-treated normal human cells and found that the cytotoxicity of CAPE was mediated by the activation of p53-growth arrest and DNA damage-inducible 45 (GADD45). Bioinformatics and experimental analyses revealed that CAPE targeted mortalin-p53 interactions, resulting in the nuclear translocation and re-activation of p53, leading to growth arrest in cancer cells (12). In the present study, we report that ARC possesses similar capabilities; however its cytotoxic efficacy is low. In order to increase the potential of ARC, we prepared the following: i) supercritical extract [green propolis supercritical extract (GPSE)]; and ii) its complex with γCD (GPSE-γCD). We then tested their cytotoxicity in human cancer cells. We report that GPSE contains 9.6% ARC and exerted cytotoxic effects at 0.5% (16.6 μM) and was equivalent to ~500 μM of pure ARC in *in vitro* toxicity assays. The extract exhibited marked anti-migratory activity. Furthermore, the *in vivo* efficacy of GPSE was significantly enhanced by its complex with γCD.

Materials and methods

Docking of mortalin and p53 with ARC. The crystal structures of human mortalin (PDB ID: 4KBO) and p53 (PDB ID: 1OLG) were obtained from Protein Data Bank (PDB) (31), while the ligand, ARC (Compound ID: 5472440) was from PubChem Compound (32) database. ArgusLab 4.0.1 (M 2004), a freely available molecular modelling, graphics and drug design package, was used for docking analyses. The structures of protein and the ligand molecules were prepared and the receptor grid around the binding site residues selected from the receptor was defined. The grid resolution was kept as 0.4 Å and an exhaustive search docking was performed. The docking process was carried out using the 'ArgusDock' docking engine, calculation type as 'Dock' and the ligand was kept in rigid mode. The scoring function used was an empirical scoring function, 'AScore', which takes into account van der Waals energy, hydrophobic component, hydrogen bond and deformation penalty. The parameter file, 'AScore.prm' was used to compute the binding energies. A total of 150 docking poses were generated, ranked according to the scoring function, and the highest scoring pose was used in further analyses.

Molecular dynamics simulations of ARC-docked mortalin and p53 structure. MD simulations were carried out using the GROMACS package (33,34). The force field Gromos43a1 (35) was used for ARC-docked mortalin structure (33,36,37). The GROMACS topology file was generated using the antechamber python parser interface (ACPYPE) script. The docked protein structure was solvated in a cubic box. Water molecules and appropriate counter-ions were added to neutralize the system. The solvated system was minimized using steepest descent and conjugate gradient methods until the force on each atom was less than 100 kJ/mol/nm. These geometry minimized systems were used for 10 nsec for carrying out isobaric (constant pressure-temperature) MD simulations. The temperature and pressure of the system was maintained at 300 K and 1 atmosphere pressure, respectively, with a time constant of 5 psec. A 2-fsec time step was used for integrating the equations of motion. Particle Mesh Ewald summation method along with periodic boundary conditions were also applied throughout to calculate the electrostatic potential between partial charges on atoms. Visual Molecular Dynamics (VMD) version 1.9.2 was used to calculate the root mean square deviations (RMSD) and hydrogen bond dynamics.

Cell culture. HT1080 (fibrosarcoma), A549 (lung carcinoma) and U2OS (osteosarcoma) human cell lines were purchased from DS Pharma Biomedical Co., Ltd., Osaka, Japan, and cultured in complete Dulbecco's modified Eagle's medium (DMEM; Life Technologies) medium using normal cell culture conditions with 10% fetal bovine serum as a supplement at 37˚C, 5% CO_2 and 95% air in a humidified incubator. The cultured cells were maintained for 6-10 passages. ARC (Wako Pure Chemical Industries, Ltd., Osaka, Japan), GPSE and GPSE:50%γCD complex were dissolved in dimethylsulfoxide (DMSO), and directly added to the cell culture medium to obtain the working concentrations (as indicated in the respective figures).

Preparation of the GPSE-50%γCD complex. The complex of green propolis supercritical extract (GPSE) with γCD was prepared by a conventional kneading method. GPSE and γCD were mixed in a small amount of water. The slurry was kneaded until it became a homogeneous paste. After freeze-drying of the paste, the GPSE-γCD complex thus obtained was used in the present study. The levels of artepillin in GPSE, and its complex with γCD, were determined by high-performance liquid chromatography (HPLC) using the Shimadzu HPLC system (LC-2010C; Shimadzu Corp., Kyoto, Japan) as previously described (38). A Phenomenex HPLC column [Luna 5u C18(2) 100A: 4.60 mm I.D. x150 mm] was used and the fractionation was performed at 40˚C using solution A: H_2O (0.5% acetic acid) and solution B: Acetonitrile with gradient program as follows: Isocratic 70% A (0-5 min), linear gradient 70% → 0% A (5-30 min); flow rate, 1 ml/min; injection volume, 10 μl. Detection was performed at 320 nm (Shimadzu HPLC system LC-2010C; Shimadzu Corp.).

Cell proliferation assay. Cytotoxicity assay was performed using 3-(4,5-dimethylthiazol-2-yl)-2, 5-diphenyltetrazolium bromide (MTT) assay (Life Technologies/Thermo Fisher Scientific, Waltham, MA, USA) in which cell viability was observed by the conversion of yellow MTT by the mitochondrial dehydrogenases of living cells into purple formazon (39). The statistical significance of the results was determined from 3-4 independent experiments including triplet or quadruplet sets in each experiment. IC_{50} values were calculated by the linear regression methods in MS excel.

Morphological observation. The cells were seeded in 12-well plates and treated with various concentrations of ARC (100-400 μM, as indicated in Fig. 2C), GPSE and GPSE-50%γCD (0.5%). Morphological changes were observed under a phase contrast microscope (Nikon Eclipse TE300; Nikon, Tokyo, Japan) after 48 h.

Colony formation assay. The cells (500 cells/well) were seeded in a 6-well plate. Following 24 h of incubation, when the cells had attached to the surface of the dish they were treated with ARC, GPSE or GPSE-50%γCD (0.1%) in culture medium (DMEM). The cultures were maintained for 10-15 days (when colonies formed in the control cultures) with a regular change of medium every 3rd day. The colonies were fixed in acetone: methanol (1:1), and stained with crystal violet (Wako Pure Chemical Industries Ltd.) at the end of experiments.

Immunofluorescence staining. The cells were seeded on glass coverslips placed in 12-well plates and treated with either ARC (300 μM), GPSE or GPSE-50%γCD (0.5%) in DMEM. After 48 h of treatment, cells were fixed in 4% paraformaldehyde in phosphate-buffered saline (PBS), permeabilized with 0.1% Triton X-100 for 10 min, blocked with 0.2% bovine serum albumin (BSA)/PBS for 1 h and incubated with specific primary antibodies including anti-mortalin (clone 088: raised in our laboratory) (3-5 μg/ml) and p53 (DO-1: SC-126) (3-5 μg/ml) (Santa Cruz Biotechnology, Santa Cruz, CA, USA) at 4˚C overnight. The cells were then incubated with either Alexa-488 or Alexa-594 conjugated secondary antibodies (1 μg/ml) (A11034 or A11032, Molecular Probes, Eugene, OR, USA) for 1 h. Counterstaining was performed with Hoechst 33342 (Sigma, St. Louis, MO, USA) in the dark for 10 min. The cells were examined on a Zeiss Axiovert 200 M microscope and analyzed using AxioVision 4.6 software (Carl Zeiss, Oberkochen, Germany).

Wound healing assay. The cells were plated in 6-well plates and allowed to make monolayers following which a scratch was made using a 100-ml pipette tip. The cells were then washed with PBS and cultured with the control or test compounds [GPSE or GPSE-50%γCD or γCD, (0.1%) as indicated in Fig. 4C]. The movement of the cells to the scratch area was followed for the following 24-48 h. Images were acquired under a phase contrast microscope (Nikon) with a X10 phase objective lens at the 0, 24 and 48 h time-points. The movement was quantitated by measuring the empty surface area in the control and test samples by ImageJ software. The results are expressed as the means ± standard deviation of the mean (SEM). Statistical significance of the data was determined using a Student's t-test. Values of $P<0.05$, $P<0.01$ and $P<0.001$ were considered to indicate significant, very significant and highly significant differences, respectively.

In vivo tumor progression. The effects of GPSE and GPSE-50%γCD on *in vivo* tumor progression were investigated in a nude mouse subcutaneous tumor xenograft model. BALB/c nude mice (4 weeks old, female, 3 mice in each group/average weight 21.8 g) were obtained from Nihon Clea (Tokyo, Japan). The animals were allowed to acclimatize in our laboratory for 1 week. The cells were injected subcutaneously ($1x10^7$ suspended in 0.2 ml of growth medium) into the abdomen of the nude mice and the tail vein ($1x10^6$ suspended in 0.2 ml of growth medium). GPSE and GPSE 50%γCD were administered (by oral gavage) every alternate day beginning at 1 day after the injection of the cells for 3 weeks. Tumor formation and the body weight of the mice were monitored every alternate day. The volume of the subcutaneous tumors was calculated as V = L x W2/2, where 'L' was the length and 'W' was the width of the tumor, respectively. Statistical significance of the data was calculated from 3 independent experiments (n=3 per experiment). All procedures were carried out in accordance with the Animal Experiment and Ethics Committee, Safety and Environment Management Division, National Institute of Advanced Industrial Science and Technology (AIST), Tsukuba, Japan.

Statistical analysis. All the experiments were performed in triplicate and data are expressed as the means ± SEM. An unpaired t-test (GraphPad Prism GraphPad Software, San Diego, CA, USA) and one-way ANOVA followed by Tukey's honestly significant difference (HSD) post hoc test were used to determine the degree of significance between the control and experimental samples. Statistical significance was defined as P-values as follows: $P<0.05$ (significant), $P<0.01$ (very significant) and $P<0.001$ (highly significant) for the t-test and $P<0.05$ for ANOVA followed by a post hoc test, as indicated in the figure legends.

Results

ARC docks into the mortalin-p53 complexes and induces the activation of p53. The interaction of mortalin and p53 occurs at N-terminal amino acids residues (253-282) of mortalin and C-terminal residues (323-337) of p53 (12,40-42). Based on this information, we docked ARC with mortalin or p53 or at mortalin-p53 complex interface. ARC interacted with the crystal structure of mortalin and p53 at the binding regions. It showed a docking score of -6.99 kcal/mol with mortalin. The docked complex exhibited multiple hydrogen bonds and hydrophobic interactions (Fig. 1A-a). The ligand formed 3 hydrogen bonds, 2 with Arg 126 and 1 with Thr 271 of mortalin, while residues Glu 132, Ala 195, Tyr 196, Thr 267, Asn 268 and Gly 269 played a role in hydrophobic interactions. The second oxygen atom of ARC formed 2 hydrogen bonds with nitrogen atoms (NH1 and NH2) of Arg 126. The third hydrogen bond was formed between the third oxygen atom of ARC and the third oxygen atom of Thr 271. Together the hydrogen bonds and hydrophobic interactions formed a stable protein-ligand complex.

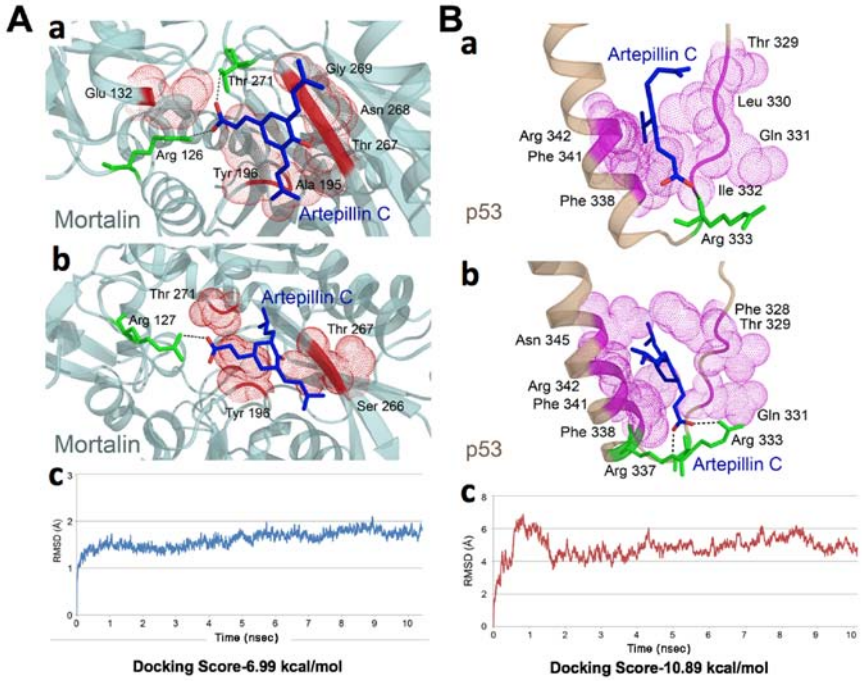

Figure 1. Artepillin C (ARC) docks into the mortalin-p53 complex. (A) Molecular docking of ARC with mortalin-p53 crystal structure (a). ARC is shown in blue, mortalin in grey and p53 in pink. Amino acids involved in the interaction are labeled in each panel. The stability of the ARC-docked mortalin structure and their RMSD trajectory (b and c) is shown. (B) Molecular docking of ARC with p53 (a). The stability of the ARC-docked p53 structure and their RMSD trajectory (b and c) is shown.

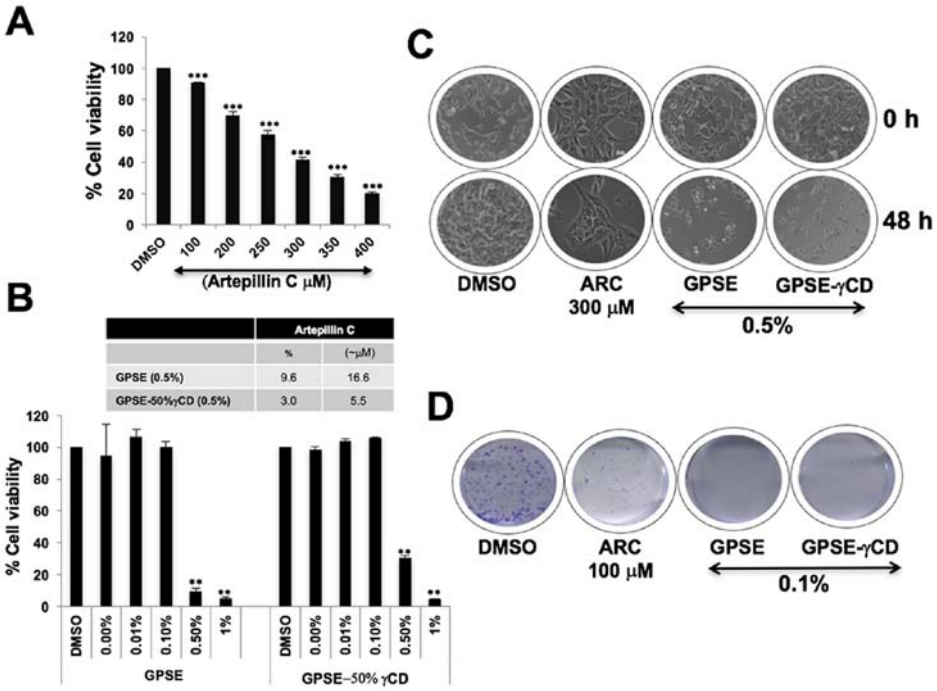

Figure 2. Cytotoxicity of artepillin C (ARC) to human cancer cells. Cell viability assay showing the (A) ARC-, and (B) GPSE and GPSE-50%γCD-induced decrease in HT1080 cell viability. (C) Cell morphology images suggesting growth arrest (in ARC-treated) and apoptosis (in GPSE- and GPSE-γCD treated) cells are shown. (D) The inhibition of colony formation in HT1080 cells in response to long-term treatment with ARC, GPSE and GPSE-γCD. GPSE and GPSE-γCD (0.1%) exerted a more potent effect than ARC (100 μM). ***P<0.001 (highly significant) and **P<0.01 (very significant) are shown as compared to the control.

The docking of ARC with p53 exhibited a score of -10.89 kcal/mol. The ligand was observed to form 1 hydrogen bond and various hydrophobic interactions (Fig. 1B-a). The nitrogen atom of Arg 333 was observed to form a hydrogen bond with the third oxygen atom of ARC. Residues Thr 329, Leu 330, Gln 331, Ile 332, Phe 338, Phe 341 and Arg 342 were involved in the hydrophobic interaction with p53. ARC docked in the cavity of p53 forming a stable complex.

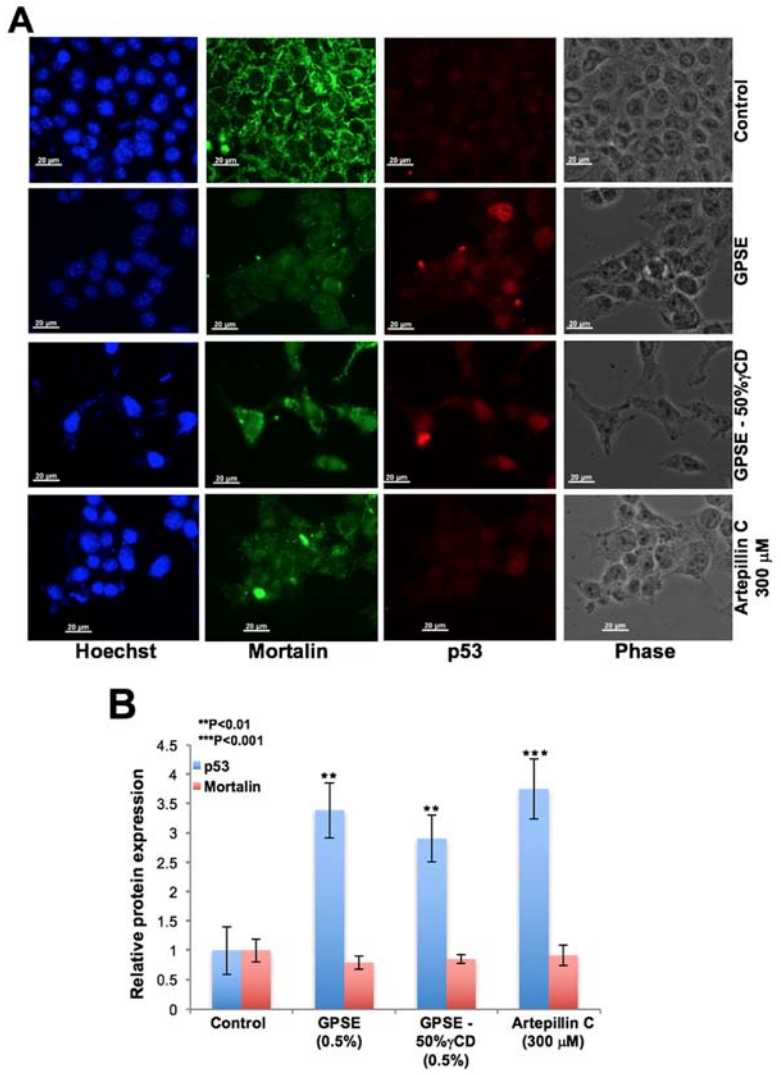

Figure 3. Artepillin C, GPSE and GPSE-γCD induce the nuclear translocation and activation of p53. (A) Immunostaining showing an increase in nuclear p53 in the cells treated with ARC, GPSE and GPSE-γCD, as compared to the control. (B) Quantification from 3 independent experiments and statistical significance is shown. Statistical significance of the data ***P<0.001 (highly significant) and **P<0.01 (very significant) are shown as compared to the control.

Molecular dynamics simulations and energy stabilization of ARC in the mortalin-p53 complex. The stability of the ARC-docked mortalin structure was further analyzed by simulating the complex for 10 nsec under conditions mimicking the bodily environment. The complex was observed to be stable for a period of 5 nsec from 5 to 10 nsec, as seen in the RMSD trajectory. Changes observed in the interacting residues of mortalin are shown in Fig. 1A-b. One hydrogen bond was observed between the oxygen atom of Arg 127 and the third oxygen atom of ARC, while residues Tyr 196, Ser 266, Thr 267 and Thr 271 were involved in hydrophobic interaction following simulations. Despite the changes in the interaction pattern of ligand-docked protein complex, the structure was more stable following simulations. The RMSD trajectory is shown Fig. 1A-c. A change in the interaction pattern of ARC docked p53 complex was observed (Fig. 1B-b). The number of hydrogen bonds between ARC and p53 increased to 2 post-simulations. One bond was formed between the second oxygen atom of ARC and nitrogen atom (NH1) of Arg 333, while the second was observed to be formed between nitrogen atom (NE) of Arg 337. The number of residues involved in hydrophobic interactions were the same, with 2 residues (Leu 330 and Ile 332) replaced with Phe 328 and Asn 345. The complex was more stable post-simulations. The ARC-docked p53 structure was observed to be stable from 5 to 10 nsec that can be seen in the RMSD trajectory (Fig. 1B-c). Bioinformatics analyses revealed that the ARC docked into the mortalin-p53 complexes (Fig. 1), similar to CAPE, and hence may cause abrogation of these complexes, and the re-activation of p53 function in cancer cells.

Anticancer activity of ARC, GPSE and the GPSE-γCD complex. We then examined the cytotoxicity of ARC in HT1080 cells and found that it induced a considerable (>20%) decrease in cell viability at concentrations of 250 μM (IC_{50}, 275 μM) (Fig. 2A). Based on such high IC_{50} values, we considered whether the extract of green propolis could be more effective than purified ARC for the reasons including that: i) it may provide a complex mixture of bioactives with multi-module action; and ii) it may protect the bioactive components from degradation. We prepared the GPSE and its conjugate with γCD (GPSE-γCD) and HPLC analyses revealed that they

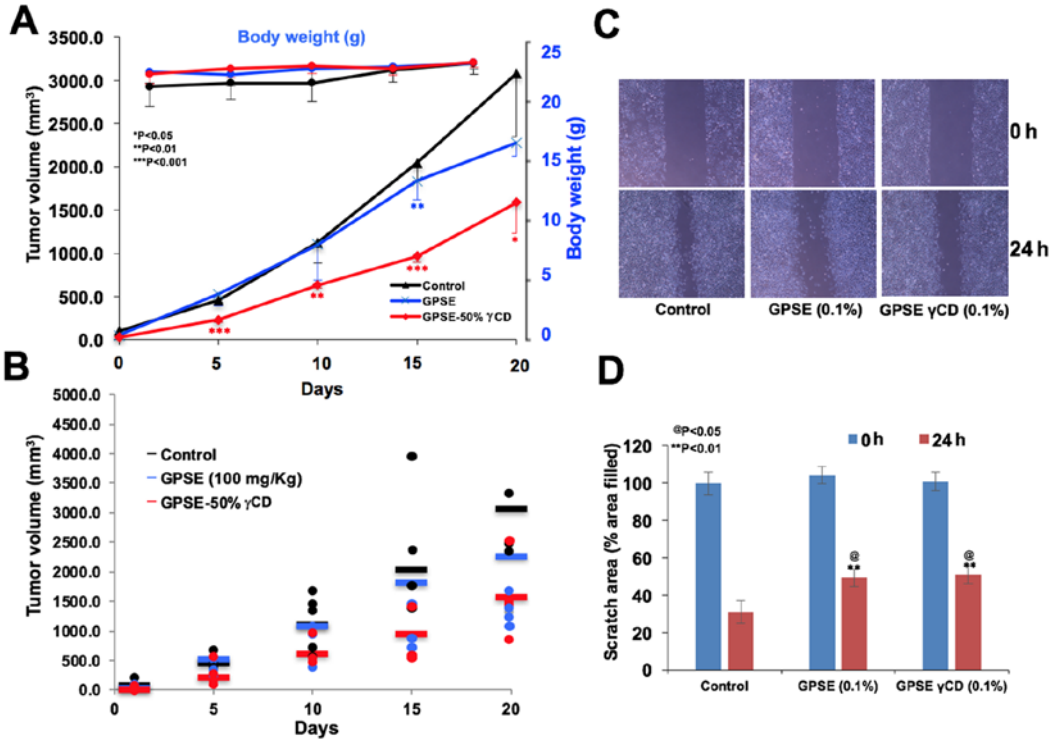

Figure 4. GPSE and GPSE-γCD possess antitumor and anti-migratory activities. (A) Nude mice treated with GPSE and GPSE-γCD showed no toxicity, as their body weight remained unaltered. (B) Inhibition of tumor growth in subcutaneous tumor xenografts was observed in mice fed GPSE and GPSE-γCD. The mice fed GPSE-γCD exhibited a greater suppression of tumor growth both in the (A) average and (B) individual mouse tumor volume analyses; n>6 from each group. (C) Wound-scratch assay revealed the anti-migratory activity of the GPSE extract which led to a slower migration rate of the treated cells into the scratch area as compared to the control. (D) Quantification of the migratory ability of the cells cultured in the control and GPSE-supplemented medium is represented as the covered area calculated from 3 experiments. Three-four independent random images were captured. The area at 0 h was taken as the control (set at 100%). Statistical significance is indicated as follows: **P<0.01, very significant as determined by the t-test and $^{@}$p<0.05, significant as determined by ANOVA followed by Tukey'shonestly significant difference (HSD) post hoc test.

contained 9.6 and 3.0% ARC, respectively. The IC_{50} values were 0.2-0.5% for GPSE and GPSE-γCD, whereas they were 250-300 μM for ARC (Fig. 2B). Similar results were obtained with the A549 and U2OS cells (data not shown). Cell morphological analysis revealed that the cytotoxicity induced by 0.5% GPSE and GPSE-γCD was comparable to that induced by 300 μM ARC (Fig. 2C). Long-term colony forming assays revealed that ARC (100 μM) induced a marked decrease in the number and size of the colonies; a more potent decrease was observed by treatment with 0.1% GPSE and GPSE-γCD (Fig. 2D).

We then examined the above-mentioned concentrations of ARC, GPSE and GPSE-γCD, and determined their effects on mortalin-p53 interactions as predicted by bioinformatics analysis (Fig. 1). In several independent experiments, we found that treatment with GPSE and ARC led to the nuclear translocation of p53 (Fig. 3A), accompanied by an increase in p53 expression (Fig. 3B). We performed antitumor assays using a subcutaneous tumor xenograft model with nude mice. As shown in Fig. 4, mice fed the GPSE or GPSE-γCD exhibited no change in body weight (Fig. 4A) or physical activity (data not shown) with respect to the control group. A reduction in tumour growth was observed in the mice fed GPSE or GPSE-γCD as compared to the control group over the 3 weeks of treatment (Fig. 4B). The tumor growth data were strongly suggestive that the GPSE-γCD induced a more marked suppressive effect on tumor growth, endorsing its potential as an antitumor natural compound. We also performed *in vitro* wound healing assays to examine whether the GPSE and GPSE-γCD extracts possess anti-migratory activity and to determine whether they can be used to inhibit cancer metastasis. As shown in Fig. 4C and D, a considerable inhibition of cell migration was detected in the cells cultured in the presence of non-toxic doses of GPSE and GPSE-γCD.

Discussion

A number of different methods have been used to extract active components from propolis, including solvent extraction, e.g., ethanol (3), water or diluted aqueous ethanol (43) and supercritical carbon dioxide extracts (8,44,45). Apart from differences in the yield due to the function of temperature, pressure and solvent concentration, the different extraction methods generate mixtures with different components and also show different activities. Supercritical extracts have non-polar characteristics that are tolerant to oxidation and provide high yields (8,44,46). However, due to their poor solubility in aqueous solvents, their use is limited in *in vitro* and *in vivo* studies. Cyclodextrins (CDs), with inner lipophilic cavities and hydrophilic outer surfaces, are capable of encapsulating molecules by non-covalent inclusion (47,48). We previously used γCD to conjugate with CAPE to generate a CAPE-γCD complex that showed significant anticancer activity (12). In the present study, we demonstrate that ARC, an active component

of Brazilian green propolis, activates p53 tumor suppressor protein by abrogating its complex with mortalin (p53 inactivating protein), and thus possesses anticancer activity. However, it turned out to be a low efficacy compound (IC_{50}, 275 μM). We hypothesized that crude extracts of green propolis may possess better efficacy. Hence, we generated its supercritical extract (GPSE) and its complex with γCD (GPSE-γCD). We herein report that the GPSE containing 9.6% ARC possesses high cytotoxicity to cancer cells, and was effective at concentrations of 0.25 to 0.5% (8.3-16.6 μM ARC). Furthermore, the GPSE-γCD complex (containing 3% ARC) exhibited greater cytotoxicity *in vitro* (0.25 to 0.5% = 2.7-5.5 μM ARC) and greater antitumor activity *in vivo*. Anti-migration assays revealed that GPSE, as well as the GPSE-50%γCD complex, at non-toxic concentrations, caused the delayed migration of cells to the scratch in wound healing assays, suggesting its potential for the treatment of metastatic cancers. Based on these data, GPSE-γCD is proposed as a Natural Efficient and Welfare (NEW) antitumor composite. Further studies are warranted to elucidate the molecular mechanism(s) of the potent anticancer activity of GPSE and its complex with γCD.

Acknowledgements

Priyanshu Bhargava is a recipient of the Ministry of Education, Culture, Sports, Science and Technology (MEXT) Scholarship, Japan. This study was supported by AIST (Japan) and DBT (Government of India) funds.

Competing interests

The authors declare that they have no competing interests.

References

1. Bankova V: Chemical diversity of propolis and the problem of standardization. J Ethnopharmacol 100: 114-117, 2005.
2. Kuropatnicki AK, Szliszka E and Krol W: Historical aspects of propolis research in modern times. Evid Based Complement Alternat Med 2013: 964149, 2013.
3. Burdock GA: Review of the biological properties and toxicity of bee propolis (propolis). Food Chem Toxicol 36: 347-363, 1998.
4. Bankova V, Popova M and Trusheva B: Propolis volatile compounds: chemical diversity and biological activity: A review. Chem Cent J 8: 28, 2014.
5. Fauzi AN, Norazmi MN and Yaacob NS: Tualang honey induces apoptosis and disrupts the mitochondrial membrane potential of human breast and cervical cancer cell lines. Food Chem Toxicol 49: 871-878, 2011.
6. Ghashm AA, Othman NH, Khattak MN, Ismail NM and Saini R: Antiproliferative effect of Tualang honey on oral squamous cell carcinoma and osteosarcoma cell lines. BMC Complement Altern Med 10: 49, 2010.
7. Khacha-ananda S, Tragoolpua K, Chantawannakul P and Tragoolpua Y: Antioxidant and anti-cancer cell proliferation activity of propolis extracts from two extraction methods. Asian Pac J Cancer Prev 14: 6991-6995, 2013.
8. Machado BA, Silva RP, Barreto GA, Costa SS, Silva DF, Brandão HN, Rocha JL, Dellagostin OA, Henriques JA, Umsza-Guez MA, *et al*: Chemical composition and biological activity of extracts obtained by supercritical extraction and ethanolic extraction of brown, green and red propolis derived from different geographic regions in Brazil. PLoS One 11: e0145954, 2016.
9. Messerli SM, Ahn MR, Kunimasa K, Yanagihara M, Tatefuji T, Hashimoto K, Mautner V, Uto Y, Hori H, Kumazawa S, *et al*: Artepillin C (ARC) in Brazilian green propolis selectively blocks oncogenic PAK1 signaling and suppresses the growth of NF tumors in mice. Phytother Res 23: 423-427, 2009.
10. Rao CV, Desai D, Simi B, Kulkarni N, Amin S and Reddy BS: Inhibitory effect of caffeic acid esters on azoxymethane-induced biochemical changes and aberrant crypt foci formation in rat colon. Cancer Res 53: 4182-4188, 1993.
11. Sawicka D, Car H, Borawska MH and Nikliński J: The anticancer activity of propolis. Folia Histochem Cytobiol 50: 25-37, 2012.
12. Wadhwa R, Nigam N, Bhargava P, Dhanjal JK, Goyal S, Grover A, Sundar D, Ishida Y, Terao K and Kaul SC: Molecular characterization and enhancement of anticancer activity of caffeic acid phenethyl ester by γ cyclodextrin. J Cancer 7: 1755-1771, 2016.
13. Gao W, Wu J, Wei J, Pu L, Guo C, Yang J, Yang M and Luo H: Brazilian green propolis improves immune function in aged mice. J Clin Biochem Nutr 55: 7-10, 2014.
14. Khayyal MT, el-Ghazaly MA and el-Khatib AS: Mechanisms involved in the antiinflammatory effect of propolis extract. Drugs Exp Clin Res 19: 197-203, 1993.
15. Wang L, Yang L, Debidda M, Witte D and Zheng Y: Cdc42 GTPase-activating protein deficiency promotes genomic instability and premature aging-like phenotypes. Proc Natl Acad Sci USA 104: 1248-1253, 2007.
16. Kujumgiev A, Tsvetkova I, Serkedjieva Y, Bankova V, Christov R and Popov S: Antibacterial, antifungal and antiviral activity of propolis of different geographic origin. J Ethnopharmacol 64: 235-240, 1999.
17. Pepeljnjak S, Jalsenjak I and Maysinger D: Flavonoid content in propolis extracts and growth inhibition of *Bacillus subtilis*. Pharmazie 40: 122-123, 1985.
18. Velikova M, Bankova V, Tsvetkova I, Kujumgiev A and Marcucci MC: Antibacterial ent-kaurene from Brazilian propolis of native stingless bees. Fitoterapia 71: 693-696, 2000.
19. Jafarzadeh Kashi TS, Kasra Kermanshahi R, Erfan M, Vahid Dastjerdi E, Rezaei Y and Tabatabaei FS: Evaluating the in vitro antibacterial effect of Iranian propolis on oral microorganisms. Iran J Pharm Res 10: 363-368, 2011.
20. Sartori G, Pesarico AP, Pinton S, Dobrachinski F, Roman SS, Pauletto F, Rodrigues LC Jr and Prigol M: Protective effect of brown Brazilian propolis against acute vaginal lesions caused by herpes simplex virus type 2 in mice: Involvement of antioxidant and anti-inflammatory mechanisms. Cell Biochem Funct 30: 1-10, 2012.
21. Choudhari MK, Haghniaz R, Rajwade JM and Paknikar KM: Anticancer activity of Indian stingless bee propolis: An in vitro study. Evid Based Complement Alternat Med 2013: 928280, 2013.
22. Benguedouar L, Boussenane HN, Wided K, Alyane M, Rouibah H and Lahouel M: Efficiency of propolis extract against mitochondrial stress induced by antineoplasic agents (doxorubicin and vinblastin) in rats. Indian J Exp Biol 46: 112-119, 2008.
23. Chen CN, Weng MS, Wu CL and Lin JK: Comparison of radical scavenging activity, cytotoxic effects and apoptosis induction in human melanoma cells by Taiwanese propolis from different sources. Evid Based Complement Alternat Med 1: 175-185, 2004.
24. Hirokawa Y, Levitzki A, Lessene G, Baell J, Xiao Y, Zhu H and Maruta H: Signal therapy of human pancreatic cancer and NF1-deficient breast cancer xenograft in mice by a combination of PP1 and GL-2003, anti-PAK1 drugs (Tyr-kinase inhibitors). Cancer Lett 245: 242-251, 2007.
25. Maruta H: Effective neurofibromatosis therapeutics blocking the oncogenic kinase PAK1. Drug Discov Ther 5: 266-278, 2011.
26. Veiga RS, De Mendonça S, Mendes PB, Paulino N, Mimica MJ, Lagareiro Netto AA, Lira IS, López BG, Negrão V and Marcucci MC: Artepillin C and phenolic compounds responsible for antimicrobial and antioxidant activity of green propolis and *Baccharis dracunculifolia* DC. J Appl Microbiol 122: 911-920, 2017.
27. Kimoto T, Arai S, Kohguchi M, Aga M, Nomura Y, Micallef MJ, Kurimoto M and Mito K: Apoptosis and suppression of tumor growth by artepillin C extracted from Brazilian propolis. Cancer Detect Prev 22: 506-515, 1998.
28. Matsuno T, Jung SK, Matsumoto Y, Saito M and Morikawa J: Preferential cytotoxicity to tumor cells of 3,5-diprenyl-4-hydroxycinnamic acid (artepillin C) isolated from propolis. Anticancer Res 17A: 3565-3568, 1997.
29. Konishi Y, Hitomi Y, Yoshida M and Yoshioka E: Absorption and bioavailability of artepillin C in rats after oral administration. J Agric Food Chem 53: 9928-9933, 2005.
30. Konishi Y: Transepithelial transport of artepillin C in intestinal Caco-2 cell monolayers. Biochim Biophys Acta 1713: 138-144, 2005.

31. Berman HM, Battistuz T, Bhat TN, Bluhm WF, Bourne PE, Burkhardt K, Feng Z, Gilliland GL, Iype L, Jain S, *et al*: The Protein Data Bank. Acta Crystallogr D Biol Crystallogr 58: 899-907, 2002.
32. Bolton EE, Wang Y, Thiessen PA and Bryant SH: Chapter 12 - PubChem: Integrated platform of small molecules and biological activities Annu Rep Comput Chem 4: 217-241, 2008.
33. Van Der Spoel D, Lindahl E, Hess B, Groenhof G, Mark AE and Berendsen HJ: GROMACS: Fast, flexible, and free. J Comput Chem 26: 1701-1718, 2005.
34. van der Spoel D, van Maaren PJ and Caleman C: GROMACS molecule & liquid database. Bioinformatics 28: 752-753, 2012.
35. Lindorff-Larsen K, Piana S, Palmo K, Maragakis P, Klepeis JL, Dror RO and Shaw DE: Improved side-chain torsion potentials for the Amber ff99SB protein force field. Proteins 78: 1950-1958, 2010.
36. van der Spoel D, Lindahl E, Hess B, Van Buuren AR, Apol E, Meulenhoff PJ, Tieleman DP, Sijbers ALTM, Feenstra KA, van Drunen R, *et al*: GROMACS user manual version 3.3, 2008. ftp://ftp.gromacs.org/pub/manual/manual-3.3.pdf.
37. van Gunsteren W, Billeter S, Eising A, Hünenberger P, Krüger P, Mark A, Scott W and Tironi I: Gromos43a1. Hochschulverlag AG an der ETH Zürich, Zürich, 1996.
38. Nobushi Y, Oikawa N, Okazaki Y, Tsutsumi S, Park YK, Kurokawa M and Yasukawa K: Determination of Artepillin-C in Brazilian propolis by HPLC with photodiode array detector. J Pharm Nutr Sci 2: 127-131, 2012.
39. Ryu J, Kaul Z, Yoon AR, Liu Y, Yaguchi T, Na Y, Ahn HM, Gao R, Choi IK, Yun CO, *et al*: Identification and functional characterization of nuclear mortalin in human carcinogenesis. J Biol Chem 289: 24832-24844, 2014.
40. Grover A, Priyandoko D, Gao R, Shandilya A, Widodo N, Bisaria VS, Kaul SC, Wadhwa R and Sundar D: Withanone binds to mortalin and abrogates mortalin-p53 complex: Computational and experimental evidence. Int J Biochem Cell Biol 44: 496-504, 2012.
41. Lu WJ, Lee NP, Kaul SC, Lan F, Poon RT, Wadhwa R and Luk JM: Mortalin-p53 interaction in cancer cells is stress dependent and constitutes a selective target for cancer therapy. Cell Death Differ 18: 1046-1056, 2011.
42. Nagpal N, Goyal S, Dhanjal JK, Ye L, Kaul SC, Wadhwa R, Chaturvedi R and Grover A: Molecular dynamics-based identification of novel natural mortalin-p53 abrogators as anticancer agents. J Recept Signal Transduct Res 37: 8-16, 2017.
43. Markiewicz-Żukowska R, Car H, Naliwajko SK, Sawicka D, Szynaka B, Chyczewski L, Isidorov V and Borawska MH: Ethanolic extract of propolis, chrysin, CAPE inhibit human astroglia cells. Adv Med Sci 57: 208-216, 2012.
44. Machado BA, Barreto GA, Costa AS, Costa SS, Silva RP, da Silva DF, Brandão HN, da Rocha JL, Nunes SB, Umsza-Guez MA, *et al*: Determination of parameters for the supercritical extraction of antioxidant compounds from green propolis using carbon dioxide and ethanol as co-solvent. PLoS One 10: e0134489, 2015.
45. Takara K, Fujita M, Matsubara M, Minegaki T, Kitada N, Ohnishi N and Yokoyama T: Effects of propolis extract on sensitivity to chemotherapeutic agents in HeLa and resistant sublines. Phytother Res 21: 841-846, 2007.
46. Akanda MJ, Sarker MZ, Ferdosh S, Manap MY, Ab Rahman NN and Ab Kadir MO: Applications of supercritical fluid extraction (SFE) of palm oil and oil from natural sources. Molecules 17: 1764-1794, 2012.
47. Szente L and Szejtli J: Highly soluble cyclodextrin derivatives: Chemistry, properties, and trends in development. Adv Drug Deliv Rev 36: 17-28, 1999.
48. Charumanee S, Okonogi S, Sirithunyalug J, Wolschann P and Viernstein H: Effect of cyclodextrin types and co-solvent on solubility of a poorly water soluble drug. Sci Pharm 84: 694-704, 2016.